



HAL
open science

CFRP with voids: ultrasonic characterization of localized porosity, acceptance criteria and mechanical characteristics

Philippe A Olivier, Benoit Mascaro, Philippe Marguerès, Francis Collombet

► **To cite this version:**

Philippe A Olivier, Benoit Mascaro, Philippe Marguerès, Francis Collombet. CFRP with voids: ultrasonic characterization of localized porosity, acceptance criteria and mechanical characteristics. 16TH INTERNATIONAL CONFERENCE ON COMPOSITE MATERIALS, Jul 2007, Kyoto, Japan. hal-04496704

HAL Id: hal-04496704

<https://hal.science/hal-04496704>

Submitted on 8 Mar 2024

HAL is a multi-disciplinary open access archive for the deposit and dissemination of scientific research documents, whether they are published or not. The documents may come from teaching and research institutions in France or abroad, or from public or private research centers.

L'archive ouverte pluridisciplinaire **HAL**, est destinée au dépôt et à la diffusion de documents scientifiques de niveau recherche, publiés ou non, émanant des établissements d'enseignement et de recherche français ou étrangers, des laboratoires publics ou privés.



CFRP WITH VOIDS: ULTRASONIC CHARACTERIZATION OF LOCALIZED POROSITY, ACCEPTANCE CRITERIA AND MECHANICAL CHARACTERISTICS

Philippe A. Olivier*, Benoît Mascaro**¹, Philippe Margueres***, Francis Collombet*
philippe.olivier@iut-tlse3.fr

* Mechanical Engineering Laboratory of Toulouse – PRO²COM – I.U.T. Paul Sabatier

** PHASE Laboratory – University of Toulouse 3

¹ ADSIP - University of Central Lancashire, Faculty of Science & Technology

Keywords: *Voids, Ultrasonic Attenuation, Localized porosity, Mechanical Properties*

Abstract

This paper synthesizes our on-going work upon voids in carbon/polymeric laminates.

The aim of this work – carried out upon two different composite systems – is twofold. The first aim is to settle void content acceptability criteria enabling also quality control costs to be reduced. This is achieved by coupling void content to mechanical characteristics and ultrasonic absorption. The void contents are both determined by resin acid digestion and image analysis.

The second aim is to start a very first study of the detection of localized porosity (e.g. in ply drop-off zones) by ultrasonic inspection. To this end a specific kind of laminate exhibiting three different void contents was autoclave-cured.

1. Voids in composites: background

Voids in composite laminates have been extensively studied for many years [1-4]. Beyond studies dealing with voids origins and growth [5] and those devoted to optimizing the pressure path of cure cycle with the aim to get void-free laminates [6], some authors have focused their work on the influence of voids upon physical [7] and mechanical properties of composites laminates [8]. Non destructive testing and ultrasonic (U.S.) inspection have been used in order to determine the void content of CFRP laminates owing to attenuation measurements. These works resulted in relationships

between the U.S. absorption coefficients (α in $\text{dB}\cdot\text{mm}^{-1}$) and void contents ($V_v\%$) [9-11]. By correlating mechanical properties (i.e. ILSS) and ultrasonic absorption coefficient, critical void contents have been defined [10-13]. Recently, this procedure has been extended to several other mechanical characteristics such as ultimate strengths in tension, bending, etc. [13].

2. Industrial Context

The qualification of composite airframe structures to comply with aviation administration requirements are known to be very expensive. Efforts have been made for several years now to reduce these costs by replacing structural testing by theoretical (or virtual) testing [14]. Nevertheless this work is deals with closer future. Indeed, its final aim is to offer some methods to reduce quality assurance testing costs. More accurately, this work examines the possibility to reduce the amount of physical and mechanical experiments performed on test pieces cured with the structural component they represent. This can be achieved by first settling and calibrating a procedure to link void content with mechanical properties owing to ultrasonic absorption measurements on some simple samples. Once it has been calibrated the procedure will enable to avoid performing the various tests on test pieces that can be submitted only to U.S. inspection and U.S. attenuation measurements from which void content and mechanical characteristics can be directly determined. Beyond this first demonstration, a special attention is paid to the detection of localized porosity.

3. Cure cycle and void contents

3.1 Manufacturing conditions

Our work on ultrasonic absorption and the effects of voids upon mechanical properties was performed on two different composite materials. The U.D. prepreg tapes used here were respectively supplied in year 1992 (carbon/epoxy T2H-EH25 - initial resin content by weight: $W_r^0 = 34\%$) and in year 2003 (carbon/polymeric T700GC-M21 – initial resin content by weight: $W_r^0 = 37.4\%$) by Hexcel-Composites France. For both materials the temperature paths always remained those recommended by the manufacturer of the prepreg. Only the pressure routes were modified in order to obtain laminates undergoing various void contents (Fig. 1). Details about the pressure path determination procedure with respect to matrix viscosity and phase changes are given in [6].

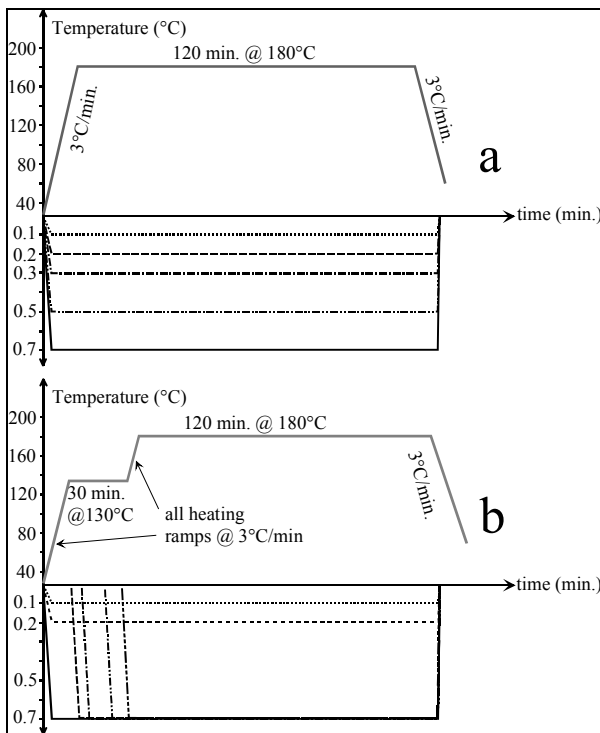


Fig. 1. (a): Temperature and pressure path for autoclave curing for T700GC-M21 laminates; (b): Idem for T2H-EH25.

3.2 Manufactured laminates and void content determination.

Table 1 gives the listing of the manufactured laminates and the mechanical properties measured.

Table 1. Listing of manufactured laminates and measured mechanical properties.

| T2H-EH25 | | <i>Measured mech. property</i> |
|--|---|--------------------------------|
| <i>V_{f0} = 60% - prepreg ply's thickness = 0.125 mm</i> | | |
| [0° ₁₆] | E ₁ , σ ₁ ^{ult.} , E ₁ ^{bend.} , σ ₁ ^{bend.} , ILSS, ν _{lt} | |
| [90° ₁₆] | E _t , σ ₁ ^{ult.} | |
| [0° ₃₂] | G _{IC} , G _{IIC} (only for void-free laminates) | |
| T700GC-M21 | | |
| <i>V_{f0} = 56% - prepreg ply's thickness = 0.256 mm</i> | | |
| [0° ₈] | E ₁ , σ ₁ ^{ult.} , E ₁ ^{bend.} , σ ₁ ^{bend.} , ILSS, C.T.E. | |
| [90° ₈] | E _t , σ ₁ ^{ult.} , C.T.E. | |
| [0° ₁₆] | G _{IC} , G _{IIC} | |
| [±45° ₄] _s | G _{lt} , τ _{lt} ^{ult.} | |

As already said, the void contents $V_v(\%)$ were determined according two methods: resin acid digestion and image analysis. Resin (or matrix) acid digestion was performed according to the specification of European standard E.N. 2564. with an absolute error of $\pm 1\%$ upon $V_v(\%)$ values.

In the mid 80's some authors [15] have shown how to use image analysis in order to determine void contents in carbon/epoxy laminates. Since 1984, numeric image techniques have undergone huge changes. Therefore it is now possible to get a much better accuracy on void content by using pictures with a large number of pixels. For each cure cycle (Fig. 1), three 30 x 30 mm x laminate's thickness samples were cut out of [0°₈], [0°₁₆] and [±45°₄]_s laminated plates. On each U.D. sample, two perpendicular edges (one \perp to fibres and one \parallel to fibres) were polished. The S.E.M. magnification was chosen as a function of the size of the largest void detected among 18 images. Then, a large number of images (up to 36 images per kind of laminate and per cure cycle) were analyzed using imageJ (Fig. 2). The best accuracy on $V_v(\%)$ determined by image analysis is of $\pm 0.3\%$.

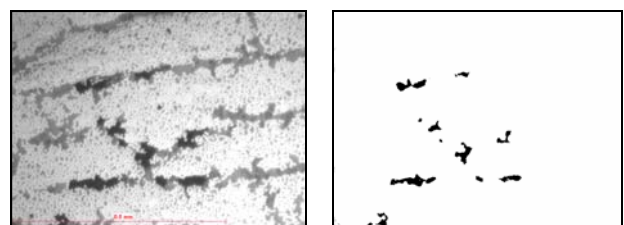


Fig. 2. Example of image treatment (before and after thresholding) for determining of void content $V_v(\%)$.

For the laminates manufactured from T700GC-M21 U.D. prepreg, the void contents

(obtained by image analysis) are given as a function of autoclave pressure in Fig. 3. This enables to assess the effects of ply orientation and changes in thickness upon $V_v(\%)$. Whatever the laminate under consideration, the differences stemming from ply orientation remain very low and this because the laminate thicknesses are not higher than 4 mm.

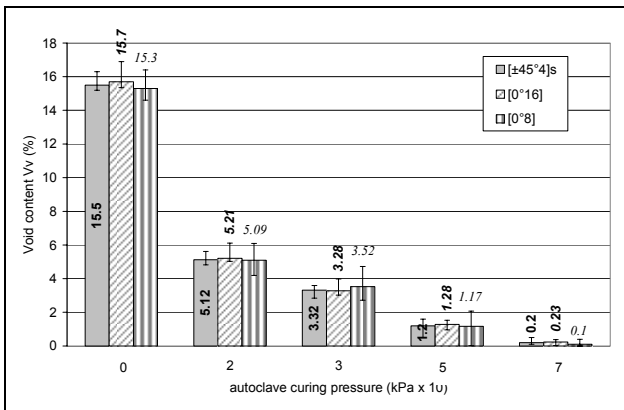


Fig. 3. Effects of pressure and ply orientation and number of ply upon void content for T700GC-M21 material.

The comparison between the two methods of $V_v(\%)$ determination is shown in Fig. 4. For low void contents (up to 5%) the two methods give very close results. But when the laminates are more porous, some surface void (i.e. void open onto samples surfaces) might distort the results. This is also true with resin acid digestion input data for which the uncertainty on cured resin specific mass can also generate some errors.

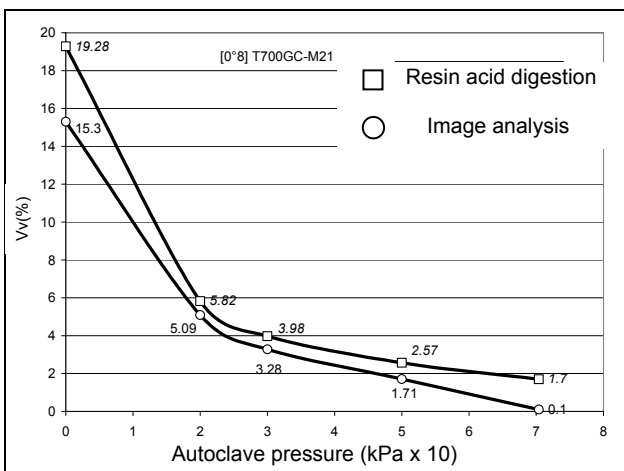


Fig. 4. Comparison between $V_v(\%)$ obtained by resin acid digestion and by image analysis on [0°/8] samples cut out from T700GC-M21 laminates as a function of autoclave pressure.

4. Effects of voids upon some mechanical properties

4.1 Tensile and in-plane shear ultimate strength

As shown in numerous papers [8-10] [17, 18] and in our previous work [6] (performed in 1995 on T2H-EH25 carbon/epoxy material) and [13] properties which are dominated by the matrix behavior are very sensitive to voids. In this study, all the mechanical tests were performed according European standards:

- ILSS: EN 2563
- Longitudinal tensile test: EN 2561;
- Transverse tensile test: EN 2597;
- In-plane shear test: EN ISO 14129;

The void contents used in this chapter 4 are those obtained by image analysis.

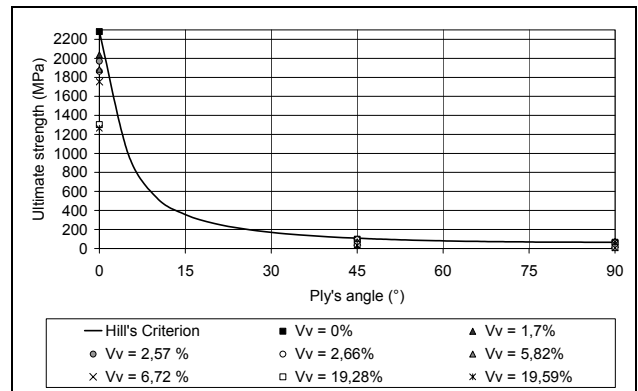


Fig. 5. Results of mechanical tensile tests: ultimate strength as functions of ply's angle and void content plotted in regards of Hill's criterion. T700GC-M21.

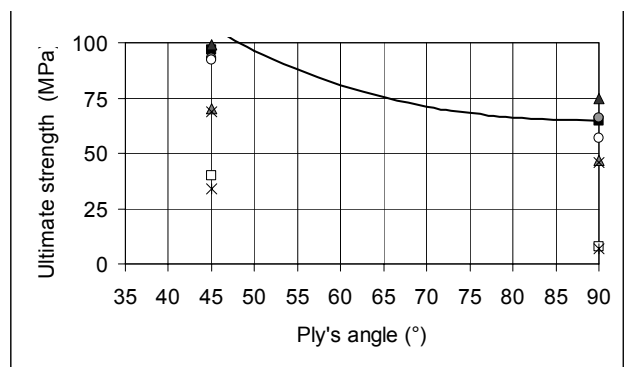


Fig. 6. Enlargement of Fig. 5 only for 45° and 90° plies.

The experimental results (ultimate strength) are plotted in Fig. 5. as functions of ply's angle (0° = longitudinal, 45° = in-plane shear, 90° = transverse) and void contents for laminates made of T700GC-

M21 material. The Hill's criterion for void-free laminates is equally plotted in Fig. 5. This enable the changes in σ_1^{ult} , σ_t^{ult} and τ_{it}^{ult} due to voids to be analysed and to evaluate the error when designing a composite structure using a failure criteria omitting voids. An enlargement of Fig. 5. for 45° and 90° laminates is given in Fig. 6 (legend unchanged).

4.1 Interlaminar shear strength (ILSS)

Fig. 7 gives the experimental results of interlaminar shear tests. The ILSS values of void-free laminates are written down in white and black. The ILSS points are fitted using a power law. This enable $V_v(\%)$ critical values to be defined. These $V_v(\%)$ critical values correspond to the first decrease recorded in ILSS using the power law fitting provided that ILSS values recorded for void-free laminates are not used for the power law fitting.

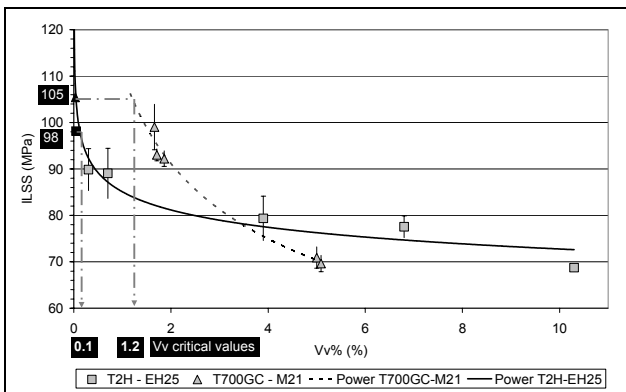


Fig. 7. Changes in ILSS as a function of $V_v(\%)$ for both materials. Fitting of exp. points by a power-law and determination of $V_v(\%)$ critical values.

4.3 Effects of voids upon G_{IC}

Mode I delamination tests were carried out according to ISO 15024. 50 mm long pre-crack were made on 0°/0° interfaces (i.e. on the mid-plane) of $[0^\circ_{16}]$ (4 mm thick) coupons. The critical strain energy release rate G_{IC} was computed according to Berry's method. It was only possible to perform mode I tests on void-free ($V_v = 0.1\%$) laminates and on laminates containing 5.09 and 15.7% voids by volume. Despite the lack of results on moderately porous laminates ($0\% < V_v < 5\%$) it can be pointed out that G_{IC} is very sensitive to voids. Effectively, a void content of 5% induces a decrease by about 22% in G_{IC} .

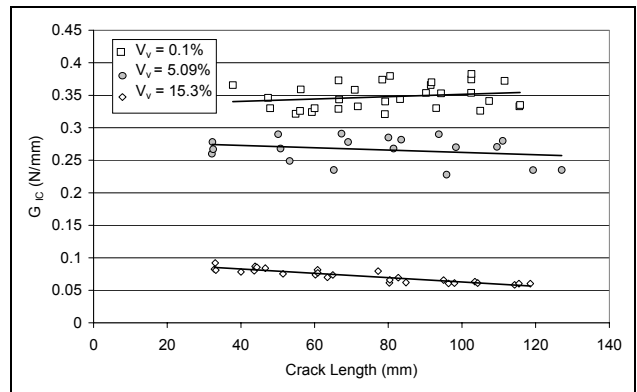


Fig. 8. Changes in G_{IC} as a function of void content for a 0°/0° interface. T700GC-M21.

4.4 Critical $V_v(\%)$ for tensile characteristics

As made for ILSS and shown in Fig.7, all the experimental points recorded in this study (i.e. σ_1^{ult} , σ_t^{ult} and τ_{it}^{ult}) were fitted using power-laws while excluding the ultimate strength values obtained on void-free laminates from these fittings. This enables void content critical value (as shown in Fig. 9. for transverse tensile strength) to be determined. The procedure was carried out for other mechanical properties (strengths and moduli) as shown in Table 2.

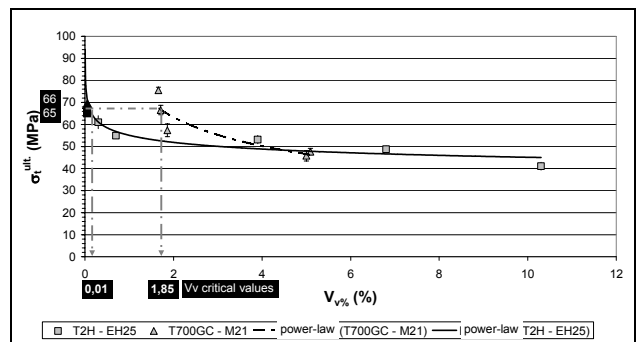


Fig. 9. Changes in σ_t^{ult} as a function of $V_v(\%)$ for both materials. Fitting of exp. points by a power-law and determination of $V_v(\%)$ critical values.

All the obtained results in terms of critical void content are gathered in Table 2 for T2H-EH25 and T700GC-M21 ultimate strength.

5. Ultrasonic study

5.1 Effects of voids upon ultrasonic attenuation

The analyses of ultrasonic signals absorption were performed in transmission on $[0^\circ_8]$ or $[0^\circ_{16}]$ for the T2H-EH25 laminates, immersed in water, using two 5 MHz transducers ($\varnothing 13$ mm).

Table 2. Mechanical testing: void content critical (or threshold) values and associated ultimate strength (in MPa) for both materials.

| $V_v(\%)$ | $\sigma_l^{ult.}$ | $\sigma_t^{ult.}$ | $ILSS$ |
|-------------------|-------------------|-------------------|--------|
| T2H-EH25 | | | |
| 0.03 | 2007 | | |
| 0.01 | | 65 | |
| 0.1 | | | 98 |
| T700GC-M21 | | | |
| 0.91 | 2282 | | |
| 1.85 | | 66 | |
| 1.2 | | | 105 |

Absorption (α) was expressed as a function of frequency (f) within the spectral bandwidth of the US emitting transducer. The absorption coefficient $\alpha(f)$ (in dB/mm) is given by (equation (1)):

$$\alpha(f) = \frac{1}{e} 10 \times \log \frac{(T \times |S_0(f)|)^2}{|S_M(f)|^2} \quad (1)$$

With: $S_0(f) = FFT(s_0(t))$;

$S_M(f) = FFT(s_M(t))$; $s_0(t)$, $s_M(t)$, signals transmitted in water and throughout material respectively (in dB); e , laminate thickness (in mm); T , coefficient of transmission at interfaces (function of acoustic impedances Z).

The absorption coefficient $\alpha(f)$ has been used in some references [8, 10-11] to characterize the void content. However, the problem is that the absorption coefficient depends on the central frequency and on the bandwidth of the emitted ultrasonic spectrum just as shown in Fig.9. Therefore, it has been chosen to use the slope of the absorption coefficient $S(\alpha) = d\alpha/df$ (in dB/mm/MHz) to characterize the voids contents. As shown by Fig. 10., the slope of the absorption coefficient is highly influenced by the void content and this for both materials under study. The relation between the changes in $S(\alpha)$ and $V_v(\%)$ is a characteristic of each material and each kind of stacking sequence. This is due to the voids shapes and size distributions which are depending on the material and on its thickness and stacking sequence.

The experimental points describing the changes in $S(\alpha)$ as a function of $V_v(\%)$ can be fitted using a power law.

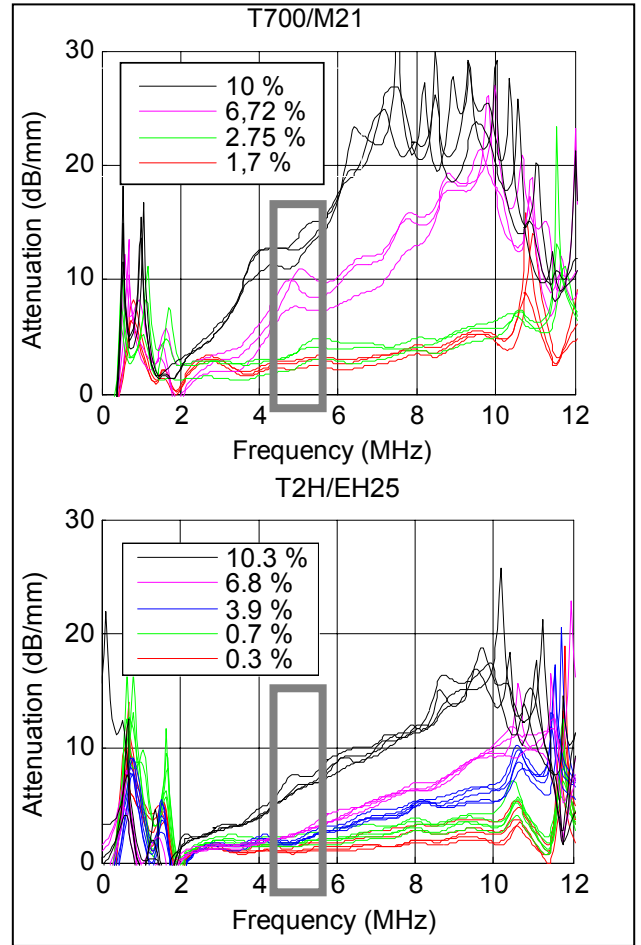


Fig. 10. Changes in ultrasonic absorption α (in dB/mm) as a function of frequency for various void contents. Top: T700GC-M21 [0°_8]. Bottom: T2H-EH25 [0°_{16}].

Generally authors use a linear fitting to link $\alpha(f)$ [10] or $S(\alpha)$ [9] to $V_v(\%)$. We have found in some references that a linear fit can lead for void-free laminates to a negative attenuation coefficient! By consequent, in order to avoid this problem, our experimental points were all fitted with power-laws. This means that if the experimental points $V_v(\%)$ versus $S(\alpha)$ are plotted in a Log-Log coordinates system the point can then be fitted using linear relations as shown here in Fig. 11. The obtained linear relations (in a Log-Log coordinates system) are directly written in Fig.10. The obtained power-laws are for respectively UD 8 and 16 plies:

$$- \text{T700GC-M21} : V_v(\%) = 2.8507 \times S(\alpha)^{0.6603} \quad (2)$$

$$- \text{T2H-EH25} : V_v(\%) = 3.9110 \times S(\alpha)^{1.7727} \quad (3)$$

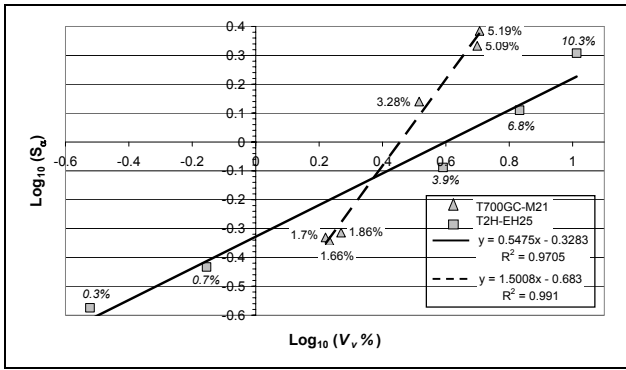


Fig. 11. Linear fit of $\text{Log}(S_\alpha)$ versus $\text{Log}(V_v\%)$ for both materials.

5.2 Relations between the slope of ultrasonic attenuation and the mechanical properties

Results of Fig. 11. and their associated equations (2) and (3) enable to correlate the experimental mechanical data (such as those given in Fig. 8 and Fig. 9 for ILSS and $\sigma_t^{\text{ult.}}$) to the slope of ultrasonic attenuation $S(\alpha)$.

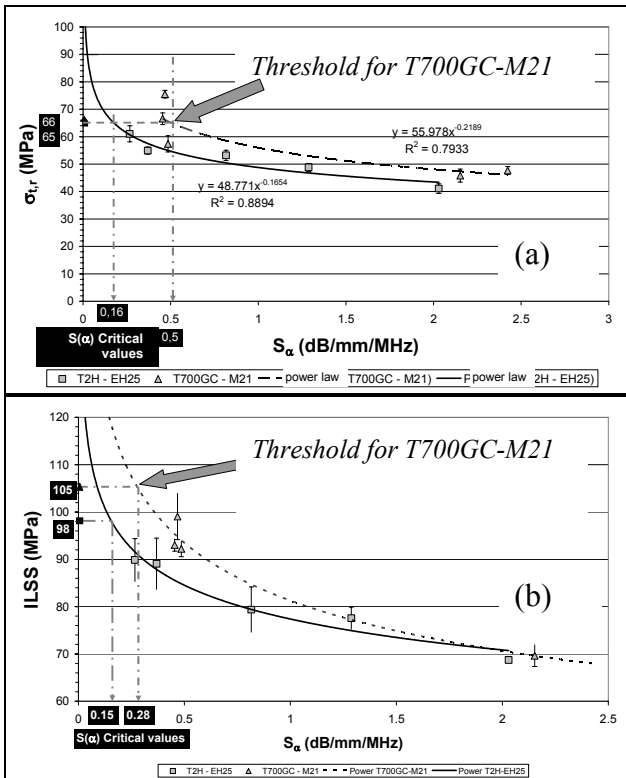


Fig. 12. (a): $\sigma_t^{\text{ult.}}$ versus $S(\alpha)$ and determination of critical $S(\alpha)$ values. (b): ILSS versus $S(\alpha)$ and determination of critical $S(\alpha)$ values.

They also enable critical (or threshold) values of $S(\alpha)$ to be determined either by graphical

construction (as shown in Fig. 12) or by calculation. In this latter case, equations (2) and (3) are introduced in the power-law equations describing the ultimate strengths as a function of $V_v(\%)$. The resulting equations describe the mechanical property considered as a function of its experimental value for a void-free laminate (denoted by 0 subscript) and $V_v(\%)$. These equations are given hereafter in Table 3.

6. Criteria for void acceptability

Correlating the mechanical ultimate strength with the slope of ultrasonic attenuation enable as it has been said to determine critical values of $S(\alpha)$. In other words, these are the values of $S(\alpha)$ beyond which the mechanical property under consideration begins to decrease.

Table 3. Power laws and thresholds obtained for longitudinal and transverse tensile tests with $E_{0,l}$, $\sigma_{0,l,r}$, $E_{0,t}$, $\sigma_{0,t,r}$ reference values for void-free specimens

| Property in tension | Power laws between property and $S(\alpha)$ | S_α^{cr} (dB/mm/MHz) |
|---------------------|---|-----------------------------|
| T2H/EH25 | | |
| Longitudinal | $E_l(S_\alpha) \approx \frac{9}{10} \cdot E_{0,l} \cdot S_\alpha^{\frac{1}{100}}$ | $3 \cdot 10^{-5}$ |
| | $\sigma_{l,r}(S_\alpha) \approx \frac{55}{69} \cdot \sigma_{0,l,r} \cdot S_\alpha^{\frac{1}{18}}$ | 0.0175 |
| Transverse | $E_t(S_\alpha) \approx \frac{8}{9} \cdot E_{0,t} \cdot S_\alpha^{\frac{1}{25}}$ | 0.0589 |
| | $\sigma_{t,r}(S_\alpha) \approx \frac{17}{23} \cdot \sigma_{0,t,r} \cdot S_\alpha^{\frac{1}{6}}$ | 0.1611 |
| T700/M21 | | |
| Longitudinal | $E_l(S_\alpha) \approx \frac{10}{11} \cdot E_{0,l} \cdot S_\alpha^{\frac{1}{25}}$ | 0.0945 |
| | $\sigma_l(S_\alpha) \approx \frac{24}{29} \cdot \sigma_{0,l} \cdot S_\alpha^{\frac{4}{83}}$ | 0.0196 |
| Transverse | $E_t(S_\alpha) \approx \frac{7}{8} \cdot E_{0,t} \cdot S_\alpha^{\frac{1}{6}}$ | 0.4455 |
| | $\sigma_{t,r}(S_\alpha) \approx \frac{56}{65} \cdot \sigma_{0,t,r} \cdot S_\alpha^{\frac{7}{32}}$ | 0.5062 |

Concerning ILSS, a slightly different approach has been used. ILSS has been described not only as a function of $V_v(\%)$ (just as the other properties previously examined) but also as a function of mode II critical strain energy release rate G_{IIC} . Mode II critical strain energy release rates G_{IIC} were not studied here as a function of void content. Nevertheless, they have been determined for a $0^\circ/0^\circ$ interface on void-free $[0^\circ_{16}]$ (T700-M21) or $[0^\circ_{32}]$

(T2H-EH25) coupons by end notch flexure (ENF) tests. G_{IIC} values (measured on void-free laminates) are respectively: 0.57 N/mm for T2H-EH25 and 1.12 N/mm for T700GC-M21.

For T2H-EH25 ($G_{IIC} = 0.57$ N/mm) material the changes in ILSS can be described by:

- $\tau = \tau_0 = 98$ MPa
for laminates on which $S(\alpha)$ remains lower than the critical value of $S(\alpha)$:
 $S_{\alpha}^{cr} = 0.1565$ dB/mm/MHz or a void content lower than 0.15%.
- $\tau(S_{\alpha}) = 135.8 \cdot G_{IIC} \cdot S_{\alpha}^{\frac{7}{55}}$
for laminates on which $S_{\alpha} > S_{\alpha}^{cr}$ or for a void content higher than 0.15%.

For T700-M21 material ($G_{IIC} = 1.21$ N/mm) the changes in ILSS can be described by:

- $\tau = \tau_0 = 105$ MPa
for laminates on which $s(\alpha)$ remains lower than $S_{\alpha}^{cr} = 0.2814$ dB/mm/MHz or a void content lower than 1.24%
- $\tau(S_{\alpha}) = 6.2 \cdot G_{IIC} \cdot S_{\alpha}^{\frac{1}{3}}$,
for laminates on which $S_{\alpha} > S_{\alpha}^{cr}$ or for a void content higher than 1.24%

7. An assessment of localized porosity

It has been planned to use ultrasonic attenuation to analyze the effects of localized porosity. Effectively, some very thick laminates or some laminates with thickness changes such as ply drop-off exhibit unreinforced matrix areas in which voids can easily develop and growth.

In order to examine the possibility to use US attenuation to characterize porosity and to detect and to localize porosity inside a laminate of average thickness (> 5 mm), a specific kind of laminates was manufactured. To this end, 24 plies U.D. laminates have been autoclave-cured according to a specific procedure in order to get two sets of void-free plies and a set of plies with a high void-content as shown in Fig. 1. It can be seen that the center plies of the laminate are very porous while the upper and lower ones are respectively slightly porous and void-free.

Void content measurements have not been performed yet. Nevertheless, this laminate has been submitted to an ultrasonic inspection.

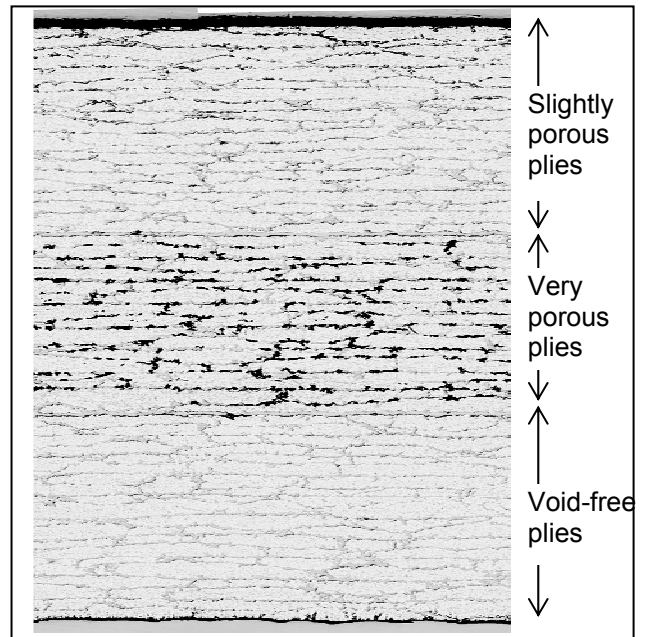


Fig. 13. Laminate with localized porosity

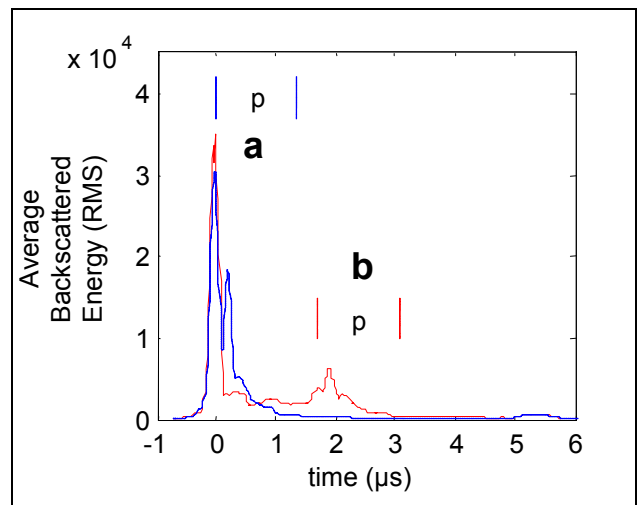


Fig. 14. Backscattered energy on a laminate in which voids are located in the top plies (a), and for a laminate with voids located in plies around the mid-plane (b).

The U.S. tests performed have shown that if a time-frequency analysis of the backscattered signals is sufficient to localize porosity in “very” porous laminates, associating time frequency analysis with backscattered energy measurements enable to localize porosity when the void content remains low. It is hoped that these very first result of our on-going

work upon voids in composite laminates could be more detailed in a future paper.

8. Concluding remarks

The changes in various physical and mechanical properties as a function of void content have been determined. An interrelation between US absorption and $V_v(\%)$ and laminates mechanical behaviour has been settled. This should contribute to reduce the quality control costs by avoiding performing some of the mechanical and chemical tests.

This study shows the feasibility of characterising the mechanical properties of composite laminates by correlating the slope of ultrasonic attenuation and the void content. Power laws have been used and determined in order to link $S(a)$ and the mechanical properties. These laws enable to define $S(\alpha)$ and $V_v(\%)$ critical values or values beyond which the voids induce a decrease in mechanical characteristics. The obtained results show the possibility to get the mechanical properties of porous laminates only by performing ultrasonic inspection and attenuation measurement. This of course, provided that the method has fully been calibrated.

Further analyses are currently performed with 3-points bending tests. However, in order to complete and improve the method described in the present paper, sets of laminates undergoing lower void contents (i.e. $V_v(\%)$ ranging from 0 and 3%) made of T700GC-M21 material have to be manufactured. In addition, the range of stacking sequences tested has to be enlarged. For the moment, $[\pm 45^{\circ}_4]_s$ laminates have not yet been submitted to US inspection. The interest is that for a given void content varying the stacking sequence may induces some changes in the void location (through the laminate thickness) and voids shapes.

9. References

- [1] Rubin A.M., Jerina K.L., « Evaluation of porosity in composite aircraft structures ». *Mechanics of Composite Materials*, Vol. 30, No 6, pp. 587-600, 1994.
- [2] Shim S.B., Seferis J.C., Hudson W. "Process induced void formation in a high performance structural composite system manufactured by autoclave lay-up processing". *Journal of Advanced Materials*, Vol. July, pp. 26-36, 1997.
- [3] Campbell F.C., Mallow A.R., Browning C.E., "Porosity in carbon fiber composites: an overview of causes". *Journal of Advanced Materials*, Vol. July, pp. 18-33, 1995.
- [4] Campbell F.C., "Manufacturing processes for advanced composites". Published by Elsevier Ltd. Oxford, UK. 2004. ISBN1856174158.
- [5] Kardos J.L., Dudukovic M.P, Dave R., "Void Growth and transport during Processing of Thermosetting-Matrix Composites". *Advances in polymer Science*, Vol. 80, pp. 101-123, 1986
- [6] Olivier P., Cottu J.P., Ferret B., "Effects of cure cycle pressure and voids on some mechanical properties of carbon/epoxy laminates". *Composites*, Vol. 26, 509-515, 1995.
- [7] H.S. Choi, K.J.Ahn, J.-D.Nam, H.J.Cun, "Hygroscopic aspects of epoxy/carbon fiber composite laminates in aircraft environments". *Composites Part A*, Vol. 32, 709-720, 2001.
- [8] Almeida S.F.M., Nogueira-Neto Z.S., "Effects of void content on the strength of composite laminates". *Composite Structures*, Vol. 28, pp. 139-148. 1994.
- [9] Jeong H., "Effects of voids on the mechanical strength ultrasonic attenuation of laminated composites". *Journal of Composite Materials*, Vol. 31, No. 3, pp. 276-292. 1997.
- [10] Costa M.L., De Almeida S.F.M. et Al., « The influence of porosity on the interlaminar shear strength of carbon/epoxy and carbon/bismaleimide fabric laminates ». *Composite Science & Technology*, Vol. 61, pp. 2101-2108. 2001.
- [11] Costa M.L., De Almeida S.F.M. et Al., « Critical void content for polymer composite laminates ». *AIAA Journal*, Vol. 43, No. 6, pp.1336-1346. 2005.
- [12] Liu, L., Zhang, B.M., et Al., "Effects of cure cycles on void content and mechanical properties of composite laminates", *Comp. Struct.*, Vol. 73, pp. 303-309. 2006.
- [13] Olivier P., Marguerès P., Mascaro B. et Al., « Assessment of the effects of voids on some physical, mechanical and damage mechanics properties of carbon/polymeric composites". *Proceedings of ECCM12*, Biarritz France, 31 August-3 September 2006, CDROM paper # 350.
- [14] Davies G.A.O, Hitchings D., "Analytical qualification of composite structures". *Proceedings of RTO – AVT Symposium on reduction of military vehicle acquisition time and cost through advanced modelling and virtual simulation*. Paris, France, 22-25 April 2002. pp. 28, 1-28,18. Published in RTO-MP 089.
- [15] Purslow D., "On the optical assessment of the void content in composite materials", *Composites*, Vol. 15, No. 3, pp. 207-210. 1984.
- [16] Santulli C, Garcia Gil R, Long AC, Clifford MJ, "Void content measurements in thermoplastic composite materials through image analysis from

optical micrographs”, *Science and Engineering of Composite Materials*, Vol. 10, p. 77-90. 2002.

- [17] Harper, B.D, Staab, G.H., Chen, R.S., “A note upon the effects of voids upon the hygral and the mechanical properties of AS4/3502 graphite epoxy”, *J. of Comp. Mat.*, Vol. 21, pp. 280-289. 1987.
- [18] Judd, N.C.W, Wright, W.W., “Void and their effects on the mechanical properties of composites - An appraisal”, *SAMPE Journal*, February, Vol. 14, No. 1, pp.10-14. 1978.

Acknowledgements

We gratefully acknowledge Airbus France (ESWT contract #WD042292) for its financial support on voids in composites and Hexcel Composites France for material supply.

The authors would also like to thanks D.G.A. and ONERA which support this work through the PEA AMERICO research program.